SANDIA REPORT
SAND2009-6250
Unlimited Release
Printed September 2009

Plasmonic Enhanced Ultrafast Switch

Eric A. Shaner, Brandon Passmore, Todd Barrick, Tom Harris, Ganesh Subramania, and John Reno

Prepared by
Sandia National Laboratories
Albuquerque, New Mexico 87185 and Livermore, California 94550

Sandia is a multiprogram laboratory operated by Sandia Corporation,
a Lockheed Martin Company, for the United States Department of Energy's
National Nuclear Security Administration under Contract DE-AC04-94AL85000.

Sandia National Laboratories

Issued by Sandia National Laboratories, operated for the United States Department of Energy by Sandia Corporation.

Printed in the United States of America. This report has been reproduced directly from the best available copy.

Available to DOE and DOE contractors from
U.S. Department of Energy
Office of Scientific and Technical Information
P.O. Box 62
Oak Ridge, TN 37831

Telephone: (865) 576-8401
Facsimile: (865) 576-5728
E-Mail: reports@adonis.osti.gov
Online ordering: http://www.osti.gov/bridge

Available to the public from
U.S. Department of Commerce
National Technical Information Service
5285 Port Royal Rd.
Springfield, VA 22161

Telephone: (800) 553-6847
Facsimile: (703) 605-6900
E-Mail: orders@ntis.fedworld.gov
Online order: http://www.ntis.gov/help/ordermethods.asp?loc=7-4-0#online

SAND2009-6250
Unlimited Release
Printed September 2009

Plasmonic Enhanced Ultrafast Switch

Eric A. Shaner, Brandon Passmore
Semiconductor Material & Device Sciences

Todd Barrick, Ganesh Subramania
Photonic Microsystems Technology

Tom Harris, John Reno
CINT Science

Sandia National Laboratories
P.O. Box 5800
Albuquerque, New Mexico 87185-MS1415

Abstract

Ultrafast electronic switches fabricated from defective material have been used for several decades in order to produce picosecond electrical transients and TeraHertz radiation. Due to the ultrashort recombination time in the photoconductor materials used, these switches are inefficient and are ultimately limited by the amount of optical power that can be applied to the switch before self-destruction. The goal of this work is to create ultrafast (sub-picosecond response) photoconductive switches on GaAs that are enhanced through plasmonic coupling structures. Here, the plasmonic coupler primarily plays the role of being a radiation condenser which will cause carriers to be generated adjacent to metallic electrodes where they can more efficiently be collected.

CONTENTS

NOMENCLATURE

THz	TeraHertz (10^{12} Hertz)
LT-GaAs	Low temperature grown GaAs

1. BACKGROUND

1.1. Motivation

Over 20 years ago, David Auston pioneered ultrafast (sub-picosecond) photoconductive switches (which are now referred to as Auston switches) [1]. Such switches have been the cornerstone of far-infrared generation and detection since their inception. An Auston switch is simply comprised of metallic electrodes patterned on a material having sub-picosecond recombination time. Typically, the sub-picosecond recombination time is achieved by creating highly defective material. In the early days, this material was oxygen implanted silicon. Later, low temperature grown GaAs became popular (and still is) due to its short recombination time combined with high carrier velocities, low dark conductivity, and breakdown voltages similar to good crystalline GaAs. On the material front, recent progress has been made in ErAs clusters embedded in GaAs in order to achieve ultrashort recombination times.

Outside of the material improvements, there has not been a great deal of progress in improving switch performance. This is due to the fact that the high-speed switches rely primarily on the defective material upon which the switch is made, and not on the switch geometry. In our research, we have found this to be a problem, as Auston switches embedded in antennas can only produce micro watts of free space radiation. We desire to change this situation by implementing plasmonic enhanced switches that should greatly improve carrier collection (ultrafast photocurrent) that is responsible for generating radiation.

2. ACCOMPLISHMENTS

2.1: Ultrafast Switches

The primary problem with Auston switches is that, since they rely on material having sub-picosecond recombination times, carrier collection is inherently inefficient. A basic Auston switch, consisting of two metal electrodes on a semiconductor, is shown in Fig. 1. A tightly focused pulsed laser is shown incident on the area between the conductors. The voltage bias between the electrodes allows collection of a photocurrent which, when feeding an antenna structure, generates transient free-space radiation. The critical issue with these switches is that most carriers are not collected, but instead recombine at defect sites. Consider a 'slow' material with a 1ps recombination time and carrier velocity of 10^7cm/s. This equates to a travel distance of only 0.1 microns. Any carriers generated more than 0.1 microns away from the conductors do not contribute to the photocurrent. For faster materials (few 100 femtosecond recombination time), the situation is even worse. Beyond this, the conductors in the switch actually shadow the most critical generation regions around the metallic boundaries.

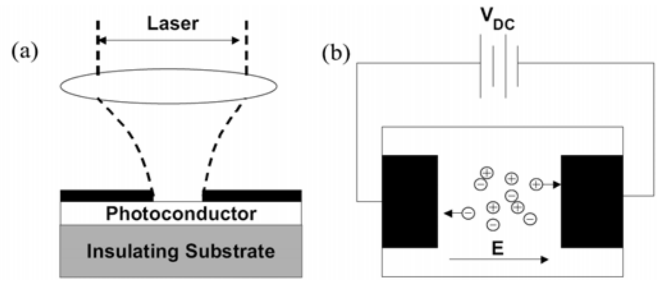

Fig. 1: The basic Auston switch. The basic illumination geometry is shown in (a). The incident laser light generates electron-hole pairs that are partially swept out of the generation region. Carriers that are not collected, due to the ultra short recombination time of the semiconductor, are lost to defect recombination.

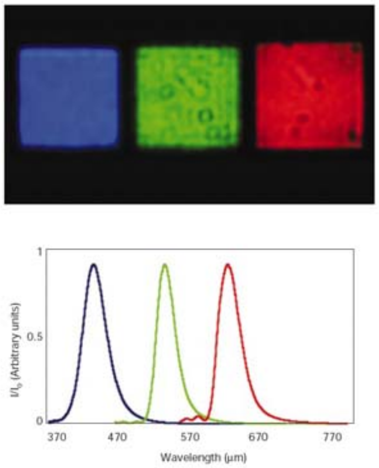

Fig. 2: Extraordinary transmission through silver film perforated with an array of holes. The blue, green, and red films have mesh hole spacing of 300, 450, and 550nm respectively. (from Barnes etal. Nature 452, 824, 2003)

Our solution is to use the surface plasmon mediated extraordinary transmission (EOT) effect of metal films perforated with arrays of sub-wavelength holes. Fig. 2 demonstrates the basic effect of film perforation. A silver film is perforated with arrays having 300nm, 450nm, and 550nm spacing. White light incident on the perforated film is transmitted within a specific band that is dependent on the hole spacing. The key point here is that the light passes through the metal. This has inspired us to develop a new photoconductive switch concept shown in Fig. 3.

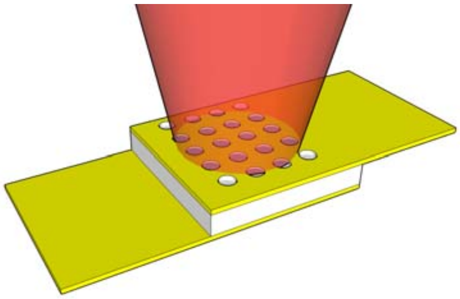

Fig. 3: Basic geometry of plasmonic enhanced photoconductive switch. The top and bottom of the switch are perforated with sub-wavelength holes in order to leverage the extraordinary transmission effect. Between the two conductors is a piece of absorbing semiconductor having sub-ps recombination time. To couple pump light of nominally 780nm wavelength into the switch, a mesh pitch of 650nm to 750nm would be required.

Figure 3 schematically illustrates the concept of integrating an EOT mesh with into a photoconductive switch. The concept is simple: Since light in a specific band (780nm wavelength is common in ultrafast systems) passes through the perforated metal film, carrier generation in the semiconductor will occur directly underneath the metal. As previously mentioned, the limitation of standard Auston switches is their ability to efficiently collect charge due to the short distances carriers travel before defect center recombination occurs. This design circumvents this problem as the light passes directly through the metal electrode enabling carrier generation as close to the collecting electrode as is possible over relatively large areas.

The fact that this type of switch has not already been conceived is easy to understand. For normal p-i-n photodetectors made from GaAs, such a design would not improve detector efficiency. In fact, it would actually decrease the external quantum efficiency. It is only for the particular case where photo-generated carrier collection is impeded by ultrafast recombination that we expect to see significant improvements. While this switch appears difficult to fabricate, as it involves processing both sides of the material, we have been doing this for many years using the Epoxy Bond and Etch Stop (EBASE) technique developed at Sandia [2].

Another promising switch design is shown in Fig. 4. Here the switch is made from a small diffraction grating that is separated into two pieces. In between the grating sections lies a small ultrafast semiconductor. The grating will be designed to diffract the incident 780nm pump light at 90 degrees. This condition will launch a surface wave on the modulated metal film. The surface wave, launched in this manner, will guide the light to the semiconductor region, where it will be converted to electron hole pairs that can be collected as an ultrafast photocurrent. If properly designed, the surface wave that guides light to the semiconductor core can actually continue to guide the light into

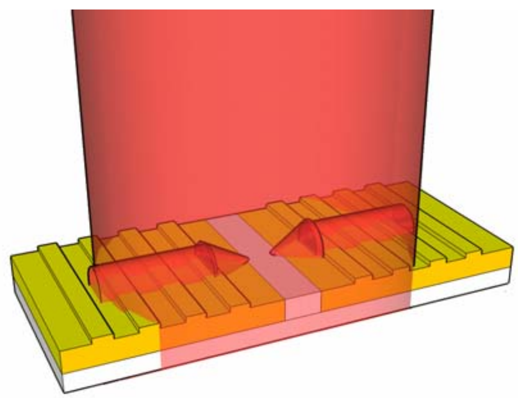

Fig. 4: Grating based photoconductive switch. The grating is designed to diffract the 780nm pump light at 90 degrees. This condition launches a surface wave on the metallic film. This surface wave will guide the light to the semiconductor absorbing region separating the two halves of the switch.

the slot between the grating sections. This could lead to a very high generation rate adjacent to the metallic electrodes and provide more of a benefit than just simply concentrating the radiation on the ultrafast material.

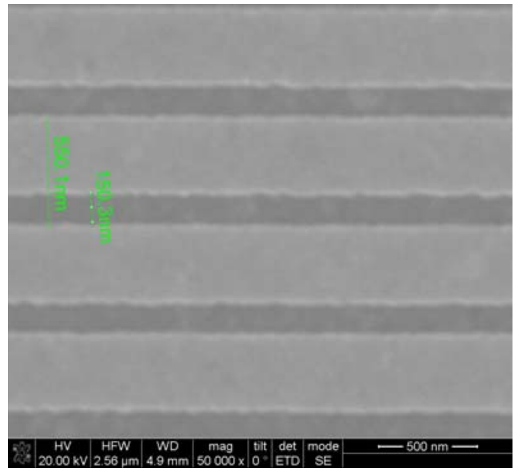

Fig. 5: Representative grating used for plasmon resonance testing. The gratings consisted of 50 nm Au corrugation on top of a planar Ti/Au 10nm/50nm film.

2.2: Plasmonic structures

Our initial investigation for palsmonic switches were centered around the perforated metal hole array concept pictured in Fig. 3. While we had become very comfortable with such structures in previous work in the mid-IR, it quickly becamse apparent that analyzing the devices on an absorbing layer (usually the substrate is non-absorbing), combined with the double-sided processign required, was going to take too long for this relatively short project. We thereafter pursued only the 1D grating concept of Fig. 4, which is a topside-only process.

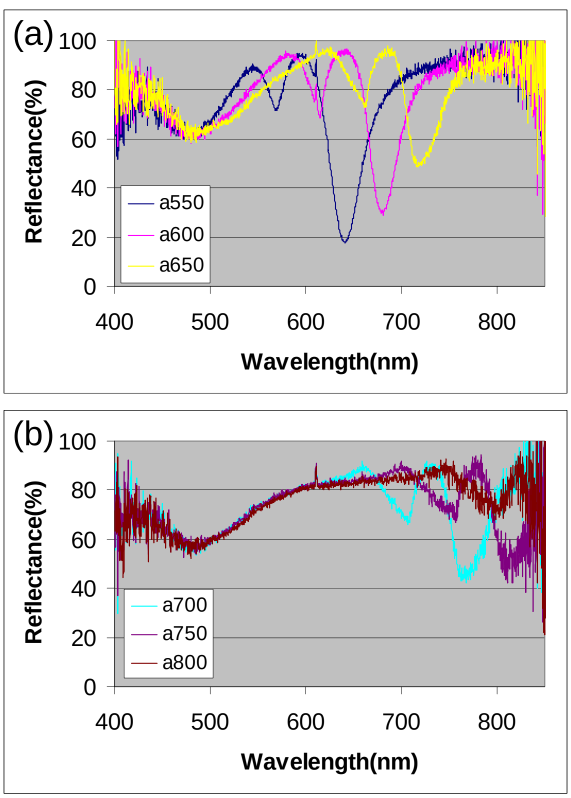

Fig. 6: Reflectance measurements of test gratings. Two reflection minima are always observed. One corresponding to a Wood's anomaly at 90 degree diffraction, always occurs at the grating period. The other, loner wavelength minima, corresponds to the surface plasmon resonance.

2.3: Tailoring the plasmonic resonance

For smooth metal films, the dispersion relation for surface plasmons is given by

$$k_{spp} = \frac{\omega}{c}\left[\frac{\varepsilon_m \varepsilon_d}{\varepsilon_m + \varepsilon_d}\right]^{\frac{1}{2}} \quad \text{Eq. 1}$$

where k_{spp} is the surface plasmon wavevector, ω is frequency, and ε_m and ε_d are the dielectric function of the metal and surrounding dielectric respectively. It turns out that free-space radiation can not couple to surface plasmons directly, but it can with the help of a grating to provide the additional momentum. In this case, the condition for surface plasmon excitation becomes

$$k_{spp} = k_{photon} \sin\theta \pm \frac{2\pi}{a_o} \text{m} \quad \text{Eq. 2}$$

where θ is the angle of incidence and a_o is the grating period.

Before making integrated plasmonic devices, we first needed to perform test runs in order to locate a plasmon resonance on a 1D grating structure that was near 780 nm (our expected operating wavelength). This was done by writing large area grating patterns on solid gold films. Since we are dealing with an air-metal plasmon mode for the device of Fig. 4, the substrate used for these tests was not important and we simply used mechanical grade GaAs. A representitive grating from these test runs is shown in Fig. 5.

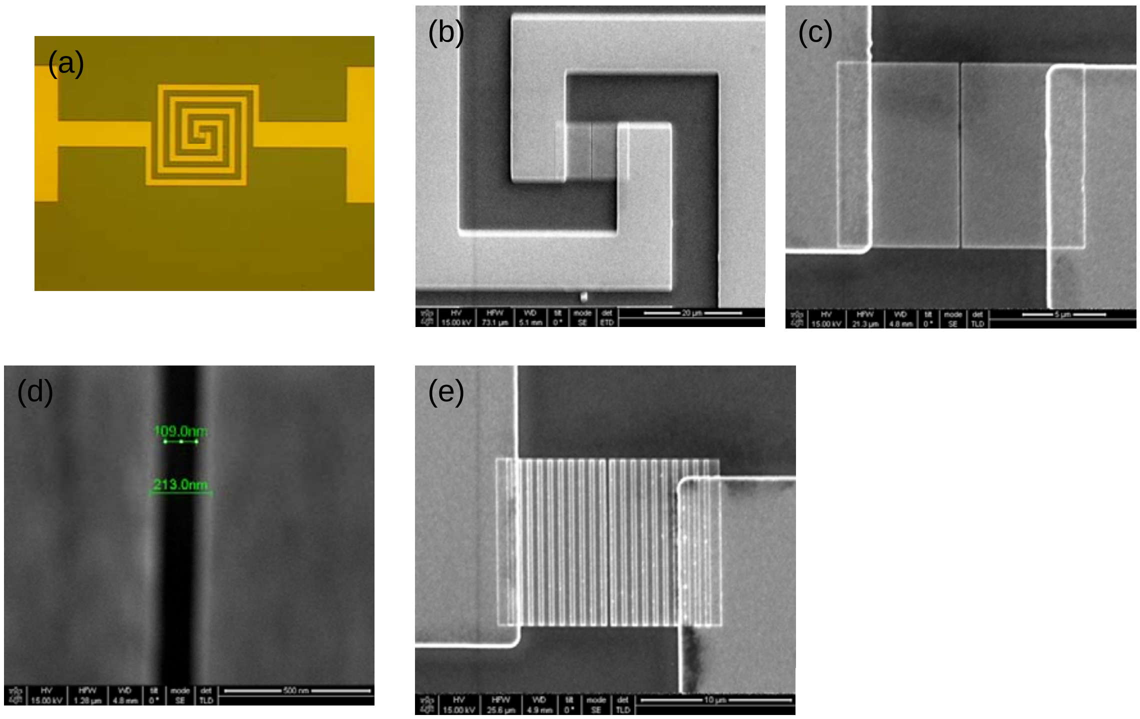

Fig. 7: Plasmonic ultrafast switches integrated with THz antennas. The broadband spiral antenna we typically implement is shown in (a). Part (b) shows a zoomed view of the interior switch region. Parts (c) and (d) show more detailed views of non-plasmonic reference switches. The plasmonic switch in part (e) is identical to the uncorrugated switch shown in (c), but it has a grating added on top with period of 700 nm.

The results of reflectance measurements for gratings of various periods is shown in Fig. 6. Here, for each period, two reflection minima are always observed. The shorter wavelength minima corresponds to the condition for 90 degree diffraction of normal incidence radiation (Wood's anomaly). The longer wavelength minima is due to the surface plasmon resonance on the grating.

It is apparent that a periodicity of around 700 nm provides a surface plasmon resonance near the desired 780 nm operating point. This being the case, we proceeded to write fully integrated test device using periods ranging from 680 nm to 720 nm. A representative ultrafast device (complete with THz free space coupling antenna) is shown in Fig. 7. The substrate for this device is comprised of a 2 micron thick LT-GaAs epilayer which was annealed at 600 degrees celcius for 30 seconds in order to have a reduced lifetime of approxaimtately 1.2 picoseconds. To make a photoconductive switch element, the grating needs to have a slot defined in the center to allow radiation coupling into the underlying semiconductor. This is done in the first ebeam writing step where slots on the order of 100 nm to 200 nm (Fig. 7(c,d)) are defined. Some of these are left on chip as non-plasmonic refence structures. Others are further patterned by a subsequent ebeam and liftoff process to define the gratings needed for surface plasmon excitation as shown in Fig. 7(e).

2.4: Device testing

While full device testing has not been accomplished yet, we have done extensive work to build an appropriate test apparatus. This system is comprised of a 3D motorized translation stage, optical fiber holder, and fiber coupling and back-reflection monitoring optics. The complete system is shown in Fig. 8 (a) along with representative back-reflection from a spiral antenna device (Fig. 8(b)) and photocurrent (Fig. 8(c)) taken during a single characterization scan. This flexible system will allow for polarization and wavelength sensitive switch testing, and can also be connected to a miniature spectrometer (by routing the back-reflection signal to the spectrometer) in order to individually test the switch optical response as was done for large area structures in Fig. 6.

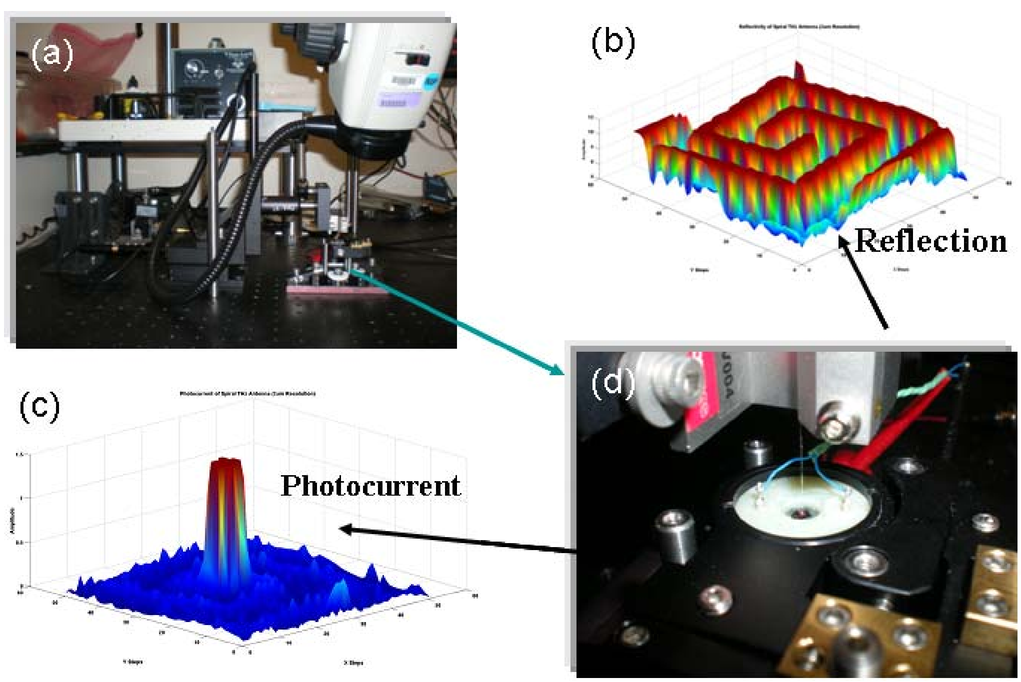

Fig. 8: Fiber based test systems. Part (a) shows the fiber setup which uses a 3D motorize stage to control optical fiber position. The reflection measurement from a spiral test antenna is shown in (b). Part (c) is the photocurrent from the same device and scan which shows a peak when illuminating the switch location in the center of the antenna. A zoomed view of the scanning fiber over a THz antenna is shown in part (d).

3. CONCLUSIONS

The work performed under this project opens some exciting paths towards future opportunities. If ultrafast photoconductive switch power generation can be improved by a factor of two or more, then this advance could strongly impact the THz community. Due to the lack of a high-power continuously tunable source in the THz, currently, continuous wave photomixers hold a niche for THz spectroscopy even though the power levels from such devices are typically 1 microwatt or less. By increasing this power figure, even moderately, the measurement time for high-resolution spectra acquired by photoconductive antennas can be greatly reduced through improved system signal-to-noise.

4. REFERENCES

1. D. H. Auston, Impulse response of photoconductors in transmission lines, IEEE J. Quantum Electron. 19, 639 (1983).
2. Weckwerth, M.V.; Simmons, J.A.; Harff, N.E.; Sherwin, M.E.; Blount, M.A.; Baca, W.E.; Chui, H.C. Epoxy bond and stop-etch (EBASE) technique enabling backside processing of (Al)GaAs heterostructures, Superlattices Microstruct, 20, 561 (1996).

Distribution

1	MS0123	D. Chavez, LDRD Office	1011
1	MS1082	Ganesh Subramania	1725
1	MS1086	Dan Barton	1123
1	MS1086	Bob Biefeld	1126
1	MS1086	Todd Barrick	1725
1	MS1303	John Reno	1132
1	MS1314	Tom Harris	1132
1	MS1415	E.A. Shaner	1123
1	MS1415	Brandon Passmore	1123
1	MS1421	J.A. Simmons	1120
1	MS1427	J.M. Phillips	1100
1	MS0899	Technical Library	9536 (electronic copy)

Sandia National Laboratories